Modelling stress-diffusion controlled phase transformations : application to stress corrosion cracking

Victor De Rancourt, Kais Ammar, Benoît Appolaire, Esteban P. Busso, Samuel Forest

CSMA 2013
11e Colloque National en Calcul des Structures
13-17 Mai 2013

Modelling Stress-Diffusion Controlled Phase Transformations: Application to Stress Corrosion Cracking

Victor de RANCOURT [1], Kais AMMAR [1], Benoît APPOLAIRE [2], Esteban BUSSO [1], Samuel FOREST [1]

[1] Mines ParisTech, Centre des Matériaux, victor.de_rancourt@mines-paristech.fr
[2] ONERA, LEM, benoit.appolaire@onera.fr

Résumé — Stress Corrosion Cracking (SCC) represents a significant cause of failure in pressurised water reactors and many efforts have been made to address this problem [1]. It involves the combined action of the environment, mechanical stresses and material properties on the damage of engineering components. Current SCC models developed to predict crack growth behaviour or SCC susceptibility criteria do not fully incorporate the complex multiphysical processes that occur during oxidation at the scale of the microstructure. The aim of the work is to formulate a multi-physics modelling framework based on continuum thermodynamics able to describe the growth of an oxide film on a polycrystalline material using the phase field method.
Mots clés — oxidation, phase field, multicomponent-diffusion, phase diagrams, multi-physics

1 Introduction

We propose a model for simulating the growth of oxide films β on γ, an austenitic iron-based alloy containing chromium. The model is based on the phase field method, which relies on the treatment of interfaces as diffuse entities of given thickness δ in contrast to sharp interface modelling. Oxidation is then seen as a phase transformation, which is modelled by the motion of diffuse interfaces. This method avoids to track interfaces as in sharp interface modelling, associated with a significant computation cost especially for complex phases morphologies in three dimensions. To this end, a continuous field ϕ is introduced as an additional degree of freedom termed as order parameter which features the following properties ; it is uniform in the bulk of each phase and varies rapidly and continuously in the interfaces.

2 Constitutive Modelling

2.1 Building of the free energy F for ternary (Fe-Cr-O) biphased systems (β-γ)

An interface free energy density noted f_ϕ and bulk free energy densities accounting for mechanics and chemistry, resp. f_σ and f_c are considered. They are assumed to depend on the following set of independent state variables $\{c_O^\beta, c_{Cr}^\beta, c_O^\gamma, c_{Cr}^\gamma, \underset{\sim}{\varepsilon}_{el}^\beta, \underset{\sim}{\varepsilon}_{el}^\gamma, \phi, \nabla\phi\}$ where c denotes molar fractions, $\underset{\sim}{\varepsilon}$ is the strain tensor and ϕ the so-called order parameter discriminating the phases. The total free energy is supposed to be :

$$F = \int_V f dV = \int_V \left(f_c + f_\sigma + f_\phi\right) dV \,. \tag{1}$$

The different couplings between the interfacial, chemical and mechanical contributions are handled by common variable dependencies :

$$f_c = f_c(c_O^\beta, c_O^\gamma, c_{Cr}^\beta, c_{Cr}^\gamma, \underset{\sim}{\varepsilon}_{el}^\beta, \underset{\sim}{\varepsilon}_{el}^\gamma, \phi)\,, \;\; f_\sigma = f_\sigma(c_O^\beta, c_O^\gamma, c_{Cr}^\beta, c_{Cr}^\gamma, \underset{\sim}{\varepsilon}_{el}^\beta, \underset{\sim}{\varepsilon}_{el}^\gamma, \phi) \text{ and } f_\phi = f_\phi(\phi, \nabla\phi)\,. \tag{2}$$

In the present work, a substitutional lattice diffusion is here assumed. Consequently, the concentration of iron can be removed from the set of state variables :

$$c_{Fe}^\alpha = 1 - c_{Cr}^\alpha - c_O^\alpha \,. \tag{3}$$

2.1.1 Interface free energy

The interface free energy is composed of a double well $g(\phi)$ and a gradient energy term such that the phase field variable ϕ is bounded above and below, with upper and lower bounds respectively 1 and 0 :

$$f_\phi = f_\phi(\phi, \nabla\phi) = 3\gamma \left(\frac{2z}{\delta} g(\phi) + \frac{\delta}{z} \parallel \nabla\phi \parallel^2 \right), \tag{4}$$

where $g(\phi) = \phi^2(1-\phi)^2$, γ is the interface energy, δ the interface thickness and $z = \ln(0.95/0.05)$. At equilibrium, when chemical and mechanical driving forces are zero, minimizing f_ϕ gives the equilibrium profile of ϕ [2] :

$$\phi^{eq}(x) = \frac{1}{2}\left(1 - \tanh\left(\frac{zx}{\delta}\right)\right). \tag{5}$$

Such profiles are used in the simulations as initial conditions for ϕ.

2.1.2 Bulk free energies, a necessary interpolation due to the diffuse interface

As shown above, the interface is attributed a non-zero volume of thickness δ. At any material point, the bulk free energy is postulated to be a mixture of the bulk free energies of the phases in contact (Fig. 1), such that this interpolated bulk energy varies from the bulk energy of β to that of γ in the diffuse interface :

$$f_c = h f_c^\beta + (1-h) f_c^\gamma \qquad \text{and} \qquad f_\sigma = h f_\sigma^\beta + (1-h) f_\sigma^\gamma \qquad \text{with} \qquad h = h(\phi) = \phi^2(3-2\phi), \tag{6}$$

The same hypothesis is made for the state variables and their dual quantities (Fig. 1) :

$$\forall i \in \{Cr, O\}, \begin{cases} c_i = h c_i^\beta + (1-h) c_i^\gamma \\ \tilde{\mu}_i = h \tilde{\mu}_i^\beta + (1-h) \tilde{\mu}_i^\gamma \end{cases} \text{and} \begin{cases} \underset{\sim}{\varepsilon} = h \underset{\sim}{\varepsilon}^\beta + (1-h) \underset{\sim}{\varepsilon}^\gamma \\ \underset{\sim}{\sigma} = h \underset{\sim}{\sigma}^\beta + (1-h) \underset{\sim}{\sigma}^\gamma \end{cases}. \tag{7}$$

It is worth stressing that this partitioning is similar to the averaging rules found in homogenisation theory in physics of heterogeneous materials. It can be noted that an "homogenisation" procedure is needed to eliminate the excessive degrees of freedom [3]. To this end, particular bounds can be chosen, i.e. Reuss-like or Voigt-like. In the present work, the following choice of bounds is done [2, 4] :

$$\forall i \in \{Cr, O\}, \tilde{\mu}_i = \tilde{\mu}_i^\beta = \tilde{\mu}_i^\gamma \qquad \text{and} \qquad \underset{\sim}{\varepsilon} = \underset{\sim}{\varepsilon}^\beta = \underset{\sim}{\varepsilon}^\gamma, \tag{8}$$

where $\tilde{\mu}_i^\alpha = \dfrac{\partial f^\alpha}{\partial c_i}$ is the diffusion potential of species i and $\underset{\sim}{\sigma}$ the stress tensor. The the sake of simpli-

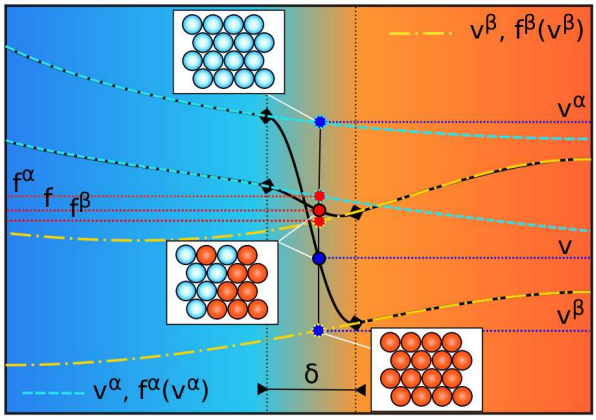

Fig. 1 – Schematic representation of the interpolation procedure of the bulk free energies and variables in the diffuse interface.

city, the chemical free energies are taken as elliptic paraboloids with respect to concentrations and the mechanical energy is given the usual quadratic form :

$$\forall \alpha \in \{\gamma, \beta\},\ f_c^\alpha = \sum_i k_i^\alpha (c_i^\alpha - c_i^{*\alpha})^2 \qquad \text{and} \qquad f_\sigma^\alpha = \underset{\sim}{\sigma}^\alpha : \underset{\sim}{\varepsilon}, \tag{9}$$

where $c_{Cr}^{*\alpha}$, $c_O^{*\alpha}$ the concentrations minimising the chemical free energy density of the phase α. c_i^α are constants fitted together with the curvatures k_i^α to recover two particular phase diagrams.

2.2 Continuum thermodynamics

2.2.1 Derivation of the balance equations using the principle of virtual power

The principle of virtual power is a straightforward way for deriving the balance equations, that will be numerically solved. It consists in multiplying work-conjugates π, $\underline{\xi}$ and $\underset{\sim}{\sigma}$ by virtual generalised velocities implying virtual powers. The virtual power of internal forces in a volume V with boundary S reads :

$$\mathscr{P}_{int}^\star = \int_V p_{int} dV = \int_V \left(\pi \phi^\star - \underline{\xi} \cdot \nabla \phi^\star - \underset{\sim}{\sigma} : \nabla \underline{u}^\star \right) dV, \tag{10}$$

We define ζ and $\underline{t}$ as respectively the external microtractions and tractions acting on the boundary surface :

$$\mathscr{P}_{ext}^\star = \int_S (\zeta \phi^\star + \underline{t} \cdot \underline{u}^\star)\, dS. \tag{11}$$

By summing external and internal virtual powers and using the properties of divergence, one obtains :

$$\int_V \left(\pi \phi^\star - \underline{\nabla} \cdot (\underline{\xi}\, \phi^\star) + \phi^\star \underline{\nabla} \cdot \underline{\xi} - \underline{\nabla} \cdot (\underset{\sim}{\sigma} \cdot \underline{u}^\star) + (\underline{\nabla} \cdot \underset{\sim}{\sigma}) \cdot \underline{u}^\star \right) dV + \int_S (\zeta \phi^\star + \underline{t} \cdot \underline{u}^\star)\, dS = 0. \tag{12}$$

Using the divergence theorem :

$$\int_V \left((\pi + \underline{\nabla} \cdot \underline{\xi}) \phi^\star + (\underline{\nabla} \cdot \underset{\sim}{\sigma}) \cdot \underline{u}^\star \right) dV + \int_S \left(\left(\zeta - \underline{\xi} \cdot \underline{n} \right) \phi^\star + \left(\underline{t} - \underset{\sim}{\sigma} \cdot \underline{n} \right) \cdot \underline{u}^\star \right) dS = 0, \tag{13}$$

where $\underline{n}$ is the unit normal vector. Because (13) is valid for every $\{\phi^\star, \underline{u}^\star\}$, the local form of the balance laws must hold :

$$\begin{cases} \pi + \underline{\nabla} \cdot \underline{\xi} = 0 & \text{for V} \\ \underline{\xi} \cdot \underline{n} = \zeta & \text{for S} \end{cases} \qquad \text{and} \qquad \begin{cases} \underline{\nabla} \cdot \underset{\sim}{\sigma} = \underline{0} & \text{for V} \\ \underset{\sim}{\sigma} \cdot \underline{n} = \underline{t} & \text{for S} \end{cases}. \tag{14}$$

The remaining balance equations are the two mass balances for O and Cr :

$$\begin{cases} \dot{c}_O = -\underline{\nabla} \cdot \underline{J}_O & \text{for V} \\ \underline{J}_O \cdot \underline{n} = j_O & \text{for S} \end{cases} \qquad \text{and} \qquad \begin{cases} \dot{c}_{Cr} = -\underline{\nabla} \cdot \underline{J}_{Cr} & \text{for V} \\ \underline{J}_{Cr} \cdot \underline{n} = j_{Cr} & \text{for S} \end{cases}. \tag{15}$$

2.2.2 First principle

Neglecting the kinetic energy for an isothermal phase transformation, the first principle of thermodynamics reads :

$$\int_V \dot{e} dV = \int_V -p_{int} dV, \tag{16}$$

where e is the internal energy density and p_{int} the total power of internal forces.

2.2.3 Second principle

The second principle of thermodynamics reads :

$$\int_V \dot{s} dV \geq \int_S \underline{\Phi} \cdot \underline{n}\, dS, \tag{17}$$

where s is the entropy density and $\underline{\Phi}$ the entropy flux. By performing a Legendre transformation, the time derivative of the free energy density can be written with respect to the time derivatives of e and s assuming that θ is homogeneous and remains constant, i.e. $\forall(\underline{X},t),\ \theta(\underline{X},t)=\theta_0$:

$$\dot{f} = \dot{e} - \theta_0 \dot{s}\,. \tag{18}$$

The second principle (17) combined with the above Legendre transformation (18) can be written in the form of the Clausius-Duhem equation for the isothermal case :

$$\int_V \left(\dot{e}-\dot{f}\right) dV \geq \theta_0 \int_S \underline{\Phi}\cdot\underline{n}\, dS\,. \tag{19}$$

2.2.4 Internal energy density, free energy density and entropy flux

To describe the internal energy, the forces acting on the system must be defined. The micro-forces and micro-stresses respectively denoted by π and $\underline{\xi}$, accounting for mass exchange and surface tension respectively, are the work-conjugate generalised velocities of the state variables ϕ and $\nabla\phi$. Hence :

$$p_{int} = \pi\dot{\phi} - \underline{\xi}\cdot\nabla\dot{\phi} - \underset{\sim}{\sigma} : \dot{\underset{\sim}{\varepsilon}}_{el}\,. \tag{20}$$

Using (16), the time derivative of the internal energy density becomes :

$$\dot{e} = -\pi\dot{\phi} + \underline{\xi}\cdot\nabla\dot{\phi} + \underset{\sim}{\sigma} : \dot{\underset{\sim}{\varepsilon}}_{el}\,. \tag{21}$$

The total time derivative of the free energy density is expanded using the chain rule :

$$\dot{f} = \frac{\partial f}{\partial c_O^\beta}\dot{c}_O^\beta + \frac{\partial f}{\partial c_{Cr}^\beta}\dot{c}_{Cr}^\beta + \frac{\partial f}{\partial c_O^\gamma}\dot{c}_O^\gamma + \frac{\partial f}{\partial c_{Cr}^\gamma}\dot{c}_{Cr}^\gamma + \frac{\partial f}{\partial \underset{\sim}{\varepsilon}_{el}} : \dot{\underset{\sim}{\varepsilon}}_{el} + \frac{\partial f}{\partial\phi}\dot{\phi} + \frac{\partial f}{\partial\nabla\phi}\cdot\nabla\dot{\phi}\,. \tag{22}$$

The entropy flux is then defined as follow using (8) :

$$\underline{\Phi} = \sum_i \frac{\tilde{\mu}_i \underline{J}_i}{\theta_0}\,. \tag{23}$$

2.2.5 Derivation of the constitutive laws

Following the solute partitioning assumption (7) the time derivative of the averaged concentration becomes :

$$\dot{c}_i = h\dot{c}_i^\beta + (1-h)\dot{c}_i^\gamma + h'\dot{\phi}(c_i^\beta - c_i^\gamma)\,. \tag{24}$$

Combining (21), (22), (24) and (23) in the Clausius-Duhem equation (19) :

$$\begin{aligned} -\left(\pi + \frac{\partial f}{\partial\phi} - h'\sum_i \tilde{\mu}_i\left(c_i^\beta - c_i^\gamma\right)\right)\dot{\phi} + \left(\underline{\xi} - \frac{\partial f}{\partial\nabla\phi}\right)\cdot\nabla\dot{\phi} + \left(\underset{\sim}{\sigma} - \frac{\partial f}{\partial \underset{\sim}{\varepsilon}^{el}}\right) : \dot{\underset{\sim}{\varepsilon}}^{el} \\ + \sum_i \left(h\left(\tilde{\mu}_i - \frac{\partial f^\beta}{\partial c_i^\beta}\right)\dot{c}_i^\beta + (1-h)\left(\tilde{\mu}_i - \frac{\partial f^\gamma}{\partial c_i^\gamma}\right)\dot{c}_i^\gamma - \underline{J}_i\cdot\nabla\tilde{\mu}_i\right) \geq 0\,, \end{aligned} \tag{25}$$

and assuming that the dissipation is independent of $\nabla\phi$, c_O^β, c_O^γ, c_{Cr}^β, c_{Cr}^γ and $\underset{\sim}{\varepsilon}_{el}$, the following constitutive laws are obtained :

$$\underline{\xi} = \frac{\partial f}{\partial\nabla\phi}, \qquad \underset{\sim}{\sigma} = \frac{\partial f}{\partial \underset{\sim}{\varepsilon}^{el}} \qquad \text{and} \qquad \tilde{\mu}_i = \frac{\partial f^\beta}{\partial c_i^\beta} = \frac{\partial f^\gamma}{\partial c_i^\gamma}\,. \tag{26}$$

2.2.6 Derivation of the complementary laws

Simplifying the Clausius-Duhem equation with the constitutive laws gives :

$$-\left(\pi+\frac{\partial f}{\partial \phi}-h'\sum_i \tilde{\mu}_i\left(c_i^\beta-c_i^\gamma\right)\right)\dot{\phi}-\sum_i \underline{J}_i\cdot\nabla\tilde{\mu}_i\geq 0\,. \tag{27}$$

The dissipative force π_{dis} is defined as :

$$\pi_{dis}=\pi+\frac{\partial f}{\partial \phi}-h'\sum_i \tilde{\mu}_i\left(c_i^\beta-c_i^\gamma\right)\,. \tag{28}$$

The dissipation equations are then obtained by introducing diffusion and interface positive mobilities, respectively L_i and M_ϕ, into the dissipation potential Ω, assumed quadratic :

$$\Omega=-\frac{L_i}{2}\parallel\nabla\tilde{\mu}_i\parallel^2-\frac{M_\phi}{2}\pi_{dis}^2\,, \tag{29}$$

Thus :

$$\underline{J}_i=\frac{\partial\Omega}{\partial\nabla\mu}=-L_i\nabla\tilde{\mu}_i \qquad \text{and} \qquad \dot{\phi}=\frac{\partial\Omega}{\partial\pi_{dis}}=-M_\phi\left(\pi+\frac{\partial f}{\partial\phi}-h\sum_{i=1}^{N}\tilde{\mu}_i(c_i^\beta-c_i^\gamma)\right)\,, \tag{30}$$

where the mobility of i is taken as a mixture of the mobilities in phases β and γ :

$$L_i=hL_i^\beta+(1-h)L_i^\gamma\,. \tag{31}$$

Furthermore, the above evolution equation for ϕ (30) can be rewritten using (14), (26) and (4) in a form where all contributions appear clearly :

$$\frac{1}{M_\phi}\dot{\phi}=\underbrace{3\gamma\left(\frac{\delta}{z}\Delta\phi-\frac{z}{\delta}g'(\phi)\right)}_{\text{interface}}-\underbrace{h'(\phi)\left(\underbrace{f_c^\beta-f_c^\gamma-\sum_i\tilde{\mu}_i(c_i^\beta-c_i^\gamma)}_{\text{chemical}}+\underbrace{f_\sigma^\beta-f_\sigma^\gamma}_{\text{mechanical}}\right)}_{\text{driving force}}\,. \tag{32}$$

The grand potential ω defined as :

$$\forall\alpha\in\{\beta,\gamma\},\ \omega^\alpha=f^\alpha-\sum_j\frac{\partial f^\alpha}{\partial c_i}c_i \qquad \text{where} \qquad f^\alpha=f_c^\alpha+f_\sigma^\alpha\,, \tag{33}$$

can be introduced in (32) to give :

$$\frac{1}{M_\phi}\dot{\phi}=\underbrace{3\gamma\left(\frac{\delta}{z}\Delta\phi-\frac{z}{\delta}g'(\phi)\right)}_{\text{interface}}-\underbrace{h'(\phi)\left(\omega^\beta-\omega^\gamma\right)}_{\text{driving force}}\,, \tag{34}$$

where the driving force is now simply the difference between the grand potentials of β and γ.

The driving force can be geometrically interpreted in Fig. 2 where the free energies of phases β and γ are plotted vs. the concentration for a binary alloy. Indeed, due to (33), the difference $\omega^\beta-\omega^\gamma$ is the vertical distance between the parallel tangents to the respective free energy curves (dashed lines). At equilibrium, the driving force vanishes, i.e. $\omega^\beta=\omega^\gamma$, and the common tangent rule (black line) is recovered.

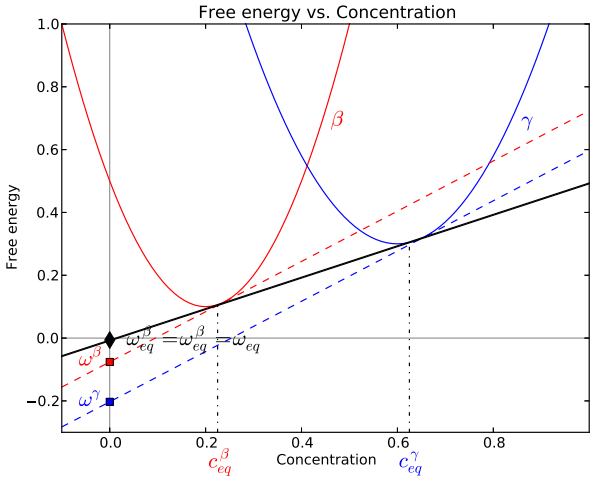

Fig. 2 – Free energy vs. concentration for a binary alloy : the parallel tangent construction

2.3 Time and space discretization of the balance equations

In this section, the balance equations are discretized using finite elements and solved with the Newton-Raphson algorithm. For this purpose, a residual vector R is henceforth defined :

$$R = \begin{pmatrix} R_\phi \\ R_{c_O} \\ R_{c_{Cr}} \\ R_{\underline{u}} \end{pmatrix}, \tag{35}$$

where R_ϕ, R_{c_O}, $R_{c_{Cr}}$ and $R_{\underline{u}}$ are the residuals of each degree of freedom which derive from the balance equations (14) and (15) :

$$\begin{array}{ll} R_\phi = \displaystyle\int_V \left(\pi\dot{\phi}^\star - \underline{\xi}\cdot\nabla\dot{\phi}^\star\right) dV + \int_S \zeta dS & R_{\underline{u}} = \displaystyle\int_V \underset{\sim}{\sigma} : \nabla\underline{\dot{u}}^\star dV + \int_S \underline{t}\, dS \\ R_{c_O} = \displaystyle\int_V (\dot{c}_O c_O^\star - \underline{J}_O\cdot\nabla c_O^\star) dV + \int_S j_O dS & R_{c_{Cr}} = \displaystyle\int_V (\dot{c}_{Cr} c_{Cr}^\star - \underline{J}_{Cr}\cdot\nabla c_{Cr}^\star) dV + \int_S j_{Cr} dS \end{array} . \tag{36}$$

The degrees of freedom ϕ, c_O, c_{Cr} and $\underline{u}$ are then spatially discretized over all finite elements containing n nodes with shape functions N. Brackets denote scalar and vector nodal values of a given degree of freedom. The matrices B and $\mathbf{B}$ are defined to compute the gradients of the scalar and vector fields.

$$\begin{array}{ll} a = N\{a\} & \nabla a = B\{a\} \\ \underline{b} = N\{\underline{b}\} & \nabla\underline{b} = \mathbf{B}\{\underline{b}\} \end{array} . \tag{37}$$

Time discretisation is carried out by finite difference :

$$\dot{a} = N(\{a\}^{t+\Delta t} - \{a\}^t)/\Delta t \qquad \text{and} \qquad \underline{\dot{b}} = N(\{\underline{b}\}^{t+\Delta t} - \{\underline{b}\}^t)/\Delta t\,. \tag{38}$$

The residuals can now be discretized :

$$\{R\} = \begin{pmatrix} \{R_\phi\} \\ \{R_{c_O}\} \\ \{R_{c_{Cr}}\} \\ \{R_{\underline{u}}\} \end{pmatrix}, \tag{39}$$

with :

$$\begin{array}{ll} \{R_\phi\} = \int_V \left(\pi N - \underline{\xi} B\right) dV + \int_S \zeta dS & \{R_{\underline{u}}\} = \int_V \underset{\sim}{\sigma} : \mathbf{B}\, dV + \int_S \underline{t}\, dS \\ \{R_{c_O}\} = \int_V (N\{\dot{c}_O\}N - \underline{J}_O B) dV + \int_S j_O dS & \{R_{c_{Cr}}\} = \int_V (N\{\dot{c}_{Cr}\}N - \underline{J}_{Cr} B) dV + \int_S j_{Cr} dS \end{array} . \tag{40}$$

The volume and surface integrals are computed using a Gauss integration procedure.

The Jacobian matrix J, which is the derivative of the vector-valued residual $\{R\}$, is written as follows :

$$J = \left[\frac{\partial R_i}{\partial s_j}\right], \tag{41}$$

where R_i is the residual of the i^{th} degree of freedom and s_j the j^{th} degree of freedom. The Jacobian matrix is updated at each time increment.

Given a desired maximum value for the residual as a convergence criterion, adaptive time stepping is applied depending on the number of necessary iterations. Furthermore an adaptive mesh refinement strategy is also applied especially to handle large 3D computations with low interface volume fractions.

3 Preliminary results in ternary alloys

Kinetic calculations involving diffusion-controlled transformations, such as oxidation, rely on a relevant description of the equilibrium phase diagram, i.e. with proper phase boundaries connected with tie-lines. If for metallic alloys, recovery of their topology is generally not a big issue, phase diagrams with oxygen involve stoichiometric compounds and features complex fan-shaped two-phase fields as show in Fig. 3, where our domain of interest ($\gamma + Cr_2O_3$) is coloured in blue. To reproduce the blue domain, the

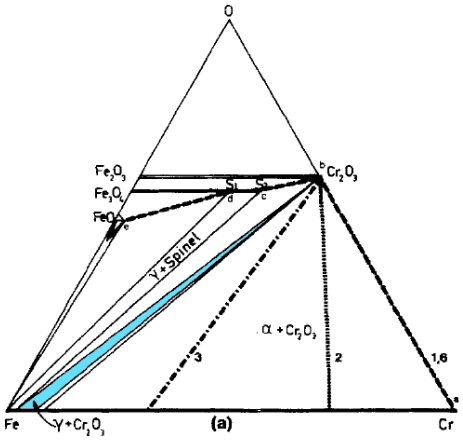

Fig. 3 – Experimental ternary diagram of Fe-Cr-O at 1200°C [6].

chemical free energy densities of phases Cr_2O_3 and Fe-γ are taken as elliptic paraboloids following (9). Large curvatures $k_{Cr}^{Cr_2O_3}$ and $k_O^{Cr_2O_3}$ have been chosen to restrict chromia to a stoichiometric compound. On the contrary, the curvature $k_{Cr}^{Fe-\gamma}$ is much smaller to extend the domain of stability of austenite to significant contents in Cr. Indeed, $k_{Cr}^{Fe-\gamma}$ is low to allow the substitution of Fe and Cr atoms. These free energy densities are shown in Fig. 4 :

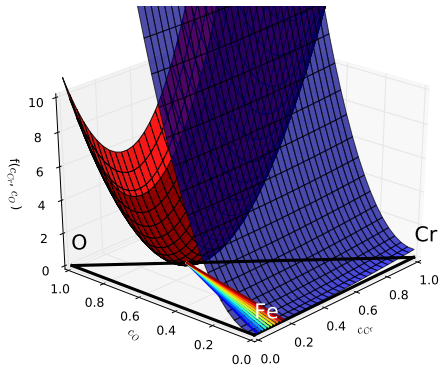

Fig. 4 – Chemical free energies of Cr_20_3 (red) and Fe-γ (blue) with the corresponding tie-lines (coloured lines), projected in the ternary section in Fig. 5

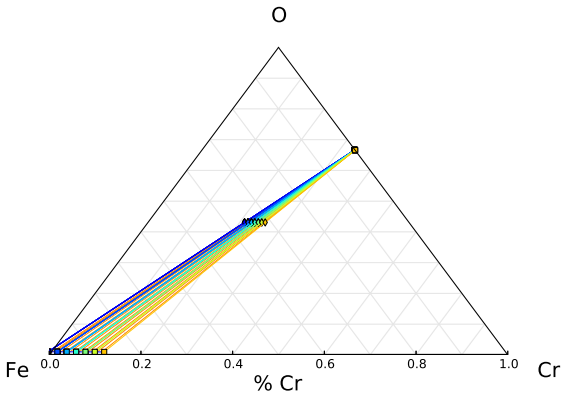

Fig. 5 – Simulated diagram (phase field method)

In multicomponent alloys, the common tangent construction to find two-phases equilibria can be generalized into a common tangent hyperplane rule. Indeed, chemical equilibrium is reached when the chemical potentials of each component are equal between phases γ and Cr_20_3 as shown in (42) :

$$\begin{array}{l} \mu_{Fe}^{Fe-\gamma}(c_{Cr}^{Fe-\gamma}, c_O^{Fe-\gamma}) = \mu_{Fe}^{Cr_2O_3}(c_{Cr}^{Cr_2O_3}, c_O^{Cr_2O_3}) \\ \mu_{Cr}^{Fe-\gamma}(c_{Cr}^{Fe-\gamma}, c_O^{Fe-\gamma}) = \mu_{Cr}^{Cr_2O_3}(c_{Cr}^{Cr_2O_3}, c_O^{Cr_2O_3}) \\ \mu_{O}^{Fe-\gamma}(c_{Cr}^{Fe-\gamma}, c_O^{Fe-\gamma}) = \mu_{O}^{Cr_2O_3}(c_{Cr}^{Cr_2O_3}, c_O^{Cr_2O_3}) \end{array} . \tag{42}$$

Solving for Eqs. (42) gives a range of tie-lines connecting the equilibrium concentrations of both phases as shown in Fig. 4. From a practical point of view, in codes devoted to the calculation of phase diagrams, each tie-line is obtained by solving Eqs. (42) supplied with overall balances involving an overall composition in the two-phase field (diamonds in Fig. 5). As shown in Fig. 5, the phase field model of section 2 with the free energies discussed above gives the expected phase diagram at equilibrium when the mechanical contribution is neglected. It is a first step toward the computation of the high temperature oxidation in Fe-Cr alloys.

4 Conclusions and prospects

We have extended a previous formulation of a phase field model incorporating elasticity and plasticity [4] to the case of multicomponent alloys, in view of its application to the oxidation of Fe-Cr alloys. Future work will focus on the computation of the oxidation process, accounting for grain boundaries as well as for dislocation enhanced bulk diffusion. Finally, the effect of stresses on the kinetics of oxidation and on the morphological evolutions will be investigated.

Références

[1] T. Couvant, L. Legras, A. Herbelin, A. Musienko, G. Ilevbrev, D. Delafosse, G. Cailletaud, and J. Hickling. Development of understanding of the interaction between localized deformation and SCC of austenitic stainless steel exposed to primary PWR environment. 2010.

[2] S. G. Kim, W. T. Kim, and T. Suzuki. Phase field model for binary alloys. *Physical Review E*, 60(6) :7186–7197, December 1999.

[3] Mathis Plapp. Unified derivation of phase-field models for alloy solidification from a grand-potential functional. *Phys. Rev. E*, 84 :031601, Sep 2011.

[4] K. Ammar, B. Appolaire, G. Cailletaud, and S. Forest. Phase field modeling of elasto-plastic deformation induced by diffusion controlled growth of a misfitting spherical precipitate. *Philosophical Magazine Letters*, 91(3) :164–172, 2011.

[5] I. Steinbach, L. Zhang, and M. Plapp. Phase field model with finite interface dissipation. *Acta Materialia*, 60 :2689–2701, 2012.

[6] M.A.J. Th Laheij, F.J.J. van Loo, and R. Metselaar. Phase relations in the Fe-Cr-O system at 1200°C investigated by means of a diffusion couple technique. *Oxidation of metals*, 14(3) :207 215, 1980.